PAPER Nr.: 72

THE INFLUENCE OF UNSTEADY AERODYNAMICS AND INTER-BLADE AERODYNAMIC COUPLING ON THE BLADES RESPONSE TO HARMONIC VARIATIONS OF THEIR PITCH ANGLES

BY

A. ROSEN, A. ISSER AND M. YOSHPE
FACULTY OF AEROSPACE ENGINEERING
TECHNION - ISRAEL INSTITUTE OF TECHNOLOGY
HAIFA 32000, ISRAEL

TWENTIETH EUROPEAN ROTORCRAFT FORUM
OCTOBER 4 - 7, 1994 AMSTERDAM

Printed by the Technical Highschool Haarlem

THE INFLUENCE OF UNSTEADY AERODYNAMICS AND INTER-BLADE AERODYNAMIC COUPLING ON THE BLADES RESPONSE TO HARMONIC VARIATIONS OF THEIR PITCH ANGLES

A. Rosen, A. Isser and M. Yoshpe
Faculty of Aerospace Engineering
Technion - Israel Institute of Technology
Haifa 32000, Israel

Abstract

During recent years a new vortex model of the unsteady aerodynamics of a hovering rotor or a rotor in axial flight, named TEMURA, has been developed in the Technion. This model has succeeded in describing various phenomena of rotor dynamics. In the present paper TEMURA is used in order to develop a model that describes the blades response to harmonic variations of their pitch angles. This model includes unsteady influences of trailing and shed vortices, together with unsteady geometric effects that represent a special capability of TEMURA. The model is general and can be applied to any number of blades and arbitrary differences between the pitch angles variations of different blades. The application of the model to analyse cases of collective harmonic pitch variations and differential harmonic pitch variations is presented. Numerical results of the new model are compared with experimental results from the literature and good agreement is shown.

1. Introduction

An accurate calculation of the dynamic response of rotor blades to harmonic variations of their pitch angles is very important in many cases that include: flight mechanics, loads calculations, vibration analysis and control. Because of its importance this subject has been investigated, quite extensively, theoretically and experimentally. A simple common approach to this problem is based on analysing the response of an isolated blade, without taking into account the inter-blade aerodynamic coupling. This approach, that appears in almost every text book on helicopter dynamics, usually includes the use of a quasi-steady blade-element (strip) aerodynamic model. When the results of such a model are compared with experimental results they exhibit large deviations in various cases. It is clear for quite a while that these deviations are the results of inter-blade aerodynamic coupling and unsteady aerodynamic effects.

A very useful method of taking into account inter-blade aerodynamic coupling and unsteady aerodynamic effects is based on the use of dynamic-inflow models. Hohenemser et al. [1,2] showed that by using a dynamic-inflow model the agreement between a calculation of the flapping response to harmonic pitch variations, and experimental results, is significantly improved (as compared to the theoretical results of a quasi-steady model). One of the earliest models of dynamic-inflow was presented in [3]. During the last twenty years dynamic-inflow models have seen a significant development. References 4-6 are examples of such developments. A detailed survey of various dynamic-inflow models and their application for the analysis of various aspects of rotor dynamics are presented in Ref. 7.

Inspite of their success in describing various phenomena of rotor dynamics, dynamic-inflow models are approximate in their nature and thus are unsuccessful in describing other phenomena.

Moreover, when dynamic inflow models are used, the description of the inter-blade aerodynamic coupling is indirect and emerges from calculations of the rotor resultant aerodynamic loads (thrust, roll and pitch moments). An effort to increase the accuracy of dynamic-inflow models [8] results in significant complications and thus two of the main advantages of these models, simplicity and ease of application, are lost.

It is clear that when it comes to accuracy, vortex models are superior to dynamic-inflow models. It was shown by various researchers that including unsteady vortex models improves the agreement between theoretical and experimental results. For example, Nagashima et al. [9] used the unsteady aerodynamic models of Loewy [10] and Miller [11] in order to analyse the aeroelastic response characteristics of a rotor executing arbitrary harmonic blade pitch variations. The use of unsteady aerodynamic models, that include inter-blade aerodynamic coupling effects, led to improved agreement between calculated and measured results. Yet, it should be noted that, inspite of their success in many cases, these unsteady models are based on various simplifying assumptions. Loewy's model, that is applied for the hovering case, is a two-dimensional model that takes into account only the shed vortices and neglects the influence of trailing vortices.

During recent years a new unsteady aerodynamic vortex model has been developed in the Technion. This model is called TEMURA (Technion Model of Unsteady Rotor Aerodynamics). It is a three-dimensional model, that takes into account shed and trailing vortices. In addition, this model also takes into account geometric effects due to perturbations in the locations of the blades (relative to the basic axisymmetric case of hovering or axial flight). The velocities that are induced over each blade include the influences of the bound vortices of this blade itself and the bound vortices of the other blades, together with the influence of the wakes behind all the blades. In this model inter-blade aerodynamic coupling is dealt with in a relatively accurate manner.

This new aerodynamic model is described in detail in [12] and parts of it has recently been described in [13,14]. In Ref. 14 the new model was used in order to calculate the flapping dynamics of the blades during pitch or roll of a hovering helicopter. The new model succeeded in predicting correctly (compared to flight test results) the off-axis response of the rotor (lateral flapping due to pitch or longitudinal flapping due to roll) and the off-axis stability derivatives (L_q and M_p). This capability is not shared by other existing models that predict an off-axis response that is opposite in direction to measured results.

The present paper describes the application of the new unsteady aerodynamic model (TEMURA) in order to calculate the dynamic response of the blades of a hovering rotor to harmonic variations of the pitch angles of the blades. The difference in terminology between pitch motion of the helicopter (that was investigated in [14]) and variations in the pitch angles of the individual blades, should be noted.

2. The Geometry of the Problem

A hovering rotor is considered. The shaft axis is fixed in space while the shaft itself rotates at a constant angular speed Ω. The rotor includes N_b identical blades. m, n and ℓ are indices that indicate the blade number ($1 \leq m,n,\ell \leq N_b$). The blade numbering is ordered in a counter clockwise direction, when looking from above.

The motion of each blade is comprised of two contributions: variation of the blade pitch angle and rigid flapping about the flapping hinge. Elastic deformations are neglected. The pitch angle variation is considered as a known input to the problem. The blade flapping is a result of aerodynamic and dynamic loads that act on each blade.

Two fixed in space (inertial) systems of coordinates are used in order to describe the spatial location of each material point of the blade, at any moment:

a) A Cartesian coordinate system (x,y,z).
b) A cylindrical coordinate system (ρ,η,z).

The origins of both systems coincide with the hub center. The z axis of the systems coincides with the shaft axis and points downward. The azimuth angle η is measured relative to the negative x direction (counter clockwise when looking from above).

The blades are represented by their mid-surface. The η coordinate of each material point on the mid-surface of blade n, at any moment τ, is described by the following sum:

$$\eta = \psi(n,\tau) + \xi \tag{2.1}$$

$\psi(n,\tau)$ is the azimuth angle of a certain representative point of the nth blade, at time τ. $\psi(n,\tau)$ will be referred to as the azimuth angle of the nth blade at time τ. Since helicopter blades have high aspect ratio and the influence of cross-sections near the root can be neglected, ξ is always very small compared to unit. $\xi_L(\rho)$ and $\xi_T(\rho)$ are the ξ coordinates of the leading-edge and trailing-edge points, respectively, of the cross-section ρ.

It is assumed that the distance between the mid-surface points and the x-y plane, as well as the angles between the normal to the mid-surface points and the z axis, are small. Thus it can also be assumed that ρ and ξ of each material point of the mid-surface do not vary with time.

The (-z) coordinate of the material point (ρ,ξ) of the mid-surface of the nth blade, at time τ, is denoted $f(n,\rho,\xi,\tau)$. ρ varies in the range $(R_a \leq \rho \leq R_b)$, where R_a and R_b are the radial coordinates of the blade root and blade tip, respectively.

If, at time τ, the flapping angle and pitch angle of the blade n, are equal to zero, then $f(n,\rho,\xi,\tau)$ is equal to $d(\rho,\xi)$. The function $d(\rho,\xi)$ defines the built-in geometry of the mid-surface.

The blade flaps about a flapping-hinge located at an offset e relative to the hub center. The flapping-hinge is normal to the blade axis (zero δ_3 angle). The pitch angle variation takes place about an axis that, in general, does not coincide with the axis $\xi=0$. At every cross-section ρ of the blade, the center of pitch variation is located at a distance $s(\rho)$ in front of the cross-sectional mid-point, that is chosen as $\xi=0$ (in fact $s(\rho)$ is the projection of this distance on the x-y plane, when the blade flapping and pitch angles are equal to zero).

The flapping and pitch angles of blade n, at time τ, are denoted $\beta(n,\tau)$ and $\theta(n,\tau)$, respectively. It is assumed that these angles are small:

$$\beta(n,\tau) \quad ; \quad \theta(n,\tau) \ll 1 \tag{2.2}$$

Based on the above assumptions it can be shown that:

$$f(\rho,\xi,n,\tau)=(\rho-e)\cdot\beta(n,\tau)+[\rho\cdot\xi-s(\rho)]\cdot\theta(n,\tau)+d(\rho,\xi) \tag{2.3}$$

The present analysis will deal with small perturbations about a basic axisymmetric state of hovering or slow axial flight (motion along the z axis direction). Thus all the variables that are associated with the problem can be described as comprised of two parts:

a) The variable in the basic state - Since the basic state is axisymmetric and all the blades are identical, the values of the variables in this state are not functions of time and do not vary between blades.

b) Small perturbations that are superimposed on the variables in the basic state - These perturbations are functions of time and vary between blades.

Thus, the value of a typical variable A - that is associated with blade n, at time τ - becomes:

$$A(\ldots,n,..,\tau,..)=\mathring{A}(\ldots)+\tilde{A}(\ldots,n,\ldots,\tau,\ldots) \tag{2.4}$$

The index $(\mathring{\ })$ refers to variables in the basic state while an upper tilde $(\tilde{\ })$ indicates a perturbation. When the perturbations are investigated it is assumed that the basic state is known and can be considered as an input to the equations of the perturbations.

Based on the above notation:

$$f(\rho,\xi,n,\tau)=\mathring{f}(\rho,\xi)+\tilde{f}(\rho,\xi,n,\tau) \tag{2.5}$$

where according to Eq. (2.3):

$$\mathring{f}(\rho,\xi)=(\rho-e)\cdot\mathring{\beta}+[\rho\cdot\xi-s(\rho)]\cdot\mathring{\theta}+d(\rho,\xi) \tag{2.6a}$$

$$\tilde{f}(\rho,\xi,n,\tau)=(\rho-e)\cdot\tilde{\beta}(n,\tau)+[\rho\cdot\xi-s(\rho)]\cdot\tilde{\theta}(n,\tau) \tag{2.6b}$$

While τ defines an arbitrary moment ($-\infty<\tau<\infty$), it is convenient to define t as the observation moment.

For the calculation of the aerodynamic geometric effects due to perturbations in the locations of the blades, a new variable $\delta f(m,r,\xi,t,n,\rho,\varphi)$, is defined:

$$\delta f(m,r,\xi,t,n,\rho,\varphi)=f(m,r,\xi,t)-f_T(n,\rho,t-\varphi/\Omega) \tag{2.7}$$

where $f_T(n,\rho,\tau)$ is the (-z) coordinate of the trailing-edge point of cross-section ρ of blade n, at time τ, namely:

$$f_T(n,\rho,\tau)\ \equiv\ f(n,\rho,\xi_T(\rho),\tau) \tag{2.8}$$

Based on the above definitions and Eqs. (2.6a,b):

$$\delta f(m,r,\xi,t,n,\rho,\varphi) = \delta \overset{\circ}{f}(r,\xi,\rho) + \delta\tilde{f}(m,r,\xi,t,n,\rho,\varphi) \qquad (2.9a)$$

$$\delta \overset{\circ}{f}(r,\xi,\rho) = (r-\rho)\cdot\overset{\circ}{\beta} + \underline{[r\cdot\xi - s(r) - \rho\cdot\xi_T(\rho) + s(\rho)]\cdot\overset{\circ}{\theta} + d(r,\xi) - d[\rho,\xi_T(\rho)]} \qquad (2.9b)$$

$$\begin{aligned}\delta\tilde{f}(m,r,\xi,t,n,\rho,\varphi) &= (r-e)\cdot\tilde{\beta}(m,t) + \underline{[r\cdot\xi - s(r)]\cdot\tilde{\theta}(m,t)} \\ &-\{(\rho-e)\cdot\tilde{\beta}(n,t-\varphi/\Omega) + \underline{[\rho\cdot\xi_T(\rho) - s(\rho)]\cdot\tilde{\theta}(n,t-\varphi/\Omega)}\}\end{aligned} \qquad (2.9c)$$

Since helicopter blades have high aspect-ratio and $d(\rho,\xi)$ is relatively small, the underlined terms in Eqs. (2.9b,c) are usually very small and thus can be neglected. Moreover, the influence of $\delta \overset{\circ}{f}(r,\xi,\rho)$ is very small in practical cases and therefore can usually be neglected.

In TEMURA harmonic perturbations are considered. In this case it is convenient to use complex numbers. Thus any perturbation variable can be described as follows:

$$\tilde{A}(\ldots,n,\ldots,\tau,\ldots) = \mathrm{Re}\left[\tilde{\tilde{A}}(\ldots,n,\ldots)\cdot e^{i\cdot\omega\cdot\tau}\right] \qquad (2.10)$$

ω is the frequency of the harmonic perturbations. All the variables associated with the problem, oscillate with the same frequency. $\tilde{\tilde{A}}(\ldots,n,\ldots)$ represents a complex amplitude (that is not a function of time, but can describe a phase shift). Based on Eq. (2.10):

$$\tilde{\beta}(n,\tau) = \mathrm{Re}\left[\tilde{\tilde{\beta}}(n)\cdot e^{i\cdot\omega\cdot\tau}\right] \qquad (2.11)$$

$$\tilde{\theta}(n,\tau) = \mathrm{Re}\left[\tilde{\tilde{\theta}}(n)\cdot e^{i\cdot\omega\cdot\tau}\right] \qquad (2.12)$$

According to Eq. (2.9c):

$$\delta\tilde{f}(m,r,\xi,t,n,\rho,\varphi) = \mathrm{Re}\left[\delta\tilde{\tilde{f}}(m,r,\xi,n,\rho,\varphi)\cdot e^{i\cdot\omega\cdot\tau}\right] \qquad (2.13)$$

where:

$$\begin{aligned}\delta\tilde{\tilde{f}}(m,r,\xi,n,\rho,\varphi) &= (r-e)\cdot\tilde{\tilde{\beta}}(m) + [r\cdot\xi - s(r)]\cdot\tilde{\tilde{\theta}}(m) \\ &-\{(\rho-e)\cdot\tilde{\tilde{\beta}}(n) + [\rho\cdot\xi_T(\rho) - s(\rho)]\cdot\tilde{\tilde{\theta}}(n)\}\cdot e^{-i\cdot k\cdot\varphi}\end{aligned} \qquad (2.14)$$

and k is the frequency ratio:

$$k = \omega/\Omega \qquad (2.15)$$

It is convenient [12-14] to replace φ by ν, according to the following equation:

$$\varphi = \nu - \psi(m,n) - [\xi - \xi_T(\rho)] \tag{2.16}$$

$\psi(m,n)$ is the azimuthal distance between blades m and n:

$$\psi(m,n) = \psi(m,\tau) - \psi(n,\tau) = 2 \cdot \pi \cdot (m-n) / N_b \tag{2.17}$$

Substitution of Eq. (2.16) into Eq. (2.14) results in:

$$\delta\tilde{\tilde{f}}(m,r,\xi,n,\rho,\varphi) \equiv \delta\tilde{\tilde{f}}(m,r,\xi,n,\rho,\nu) = (r-e)\cdot\tilde{\tilde{\beta}}(m) + [r\cdot\xi - s(r)]\cdot\tilde{\tilde{\theta}}(m)$$

$$-\left\{(\rho-e)\cdot\tilde{\tilde{\beta}}(n) + [\rho\cdot\xi_T(\rho) - s(\rho)]\cdot\tilde{\tilde{\theta}}(n)\right\} e^{-i\cdot k\cdot \nu}\cdot e^{i\cdot k\cdot\psi(m,n)}\cdot e^{i\cdot k\cdot[\xi-\xi_T(\rho)]} \tag{2.18}$$

Since high aspect-ratio blades are considered and $k \ll 10$, it can be assumed that:

$$\{k[\xi - \xi_T]\}^2 \ll 1 \tag{2.19}$$

Thus:

$$e^{i\cdot k\cdot[\xi-\xi_T(\rho)]} \cong 1 + i\cdot k\cdot[\xi - \xi_T(\rho)] \tag{2.20}$$

Substitution of Eq. (2.20) into Eq. (2.18) leads to the following expression:

$$\delta\tilde{\tilde{f}}(m,r,\xi,n,\rho,\nu) = \delta\tilde{\tilde{f}}_{F0}(m,r,n,\rho,\nu) + \xi\cdot\delta\tilde{\tilde{f}}_{F1}(m,r,n,\rho,\nu) \tag{2.21}$$

where:

$$\delta\tilde{\tilde{f}}_{F0}(m,r,n,\rho,\nu) = \mathbf{\delta f^{\beta}_{F0}}(m,r,n,\rho,\nu)\cdot\tilde{\tilde{\boldsymbol{\beta}}} + \mathbf{\delta f^{\theta}_{F0}}(m,r,n,\rho,\nu)\cdot\tilde{\tilde{\boldsymbol{\theta}}} \tag{2.22a}$$

$$\delta\tilde{\tilde{f}}_{F1}(m,r,n,\rho,\nu) = \mathbf{\delta f^{\beta}_{F1}}(m,r,n,\rho,\nu)\cdot\tilde{\tilde{\boldsymbol{\beta}}} + \mathbf{\delta f^{\theta}_{F1}}(m,r,n,\rho,\nu)\cdot\tilde{\tilde{\boldsymbol{\theta}}} \tag{2.22b}$$

$\tilde{\tilde{\boldsymbol{\beta}}}$ and $\tilde{\tilde{\boldsymbol{\theta}}}$ are column vectors of order N_b:

$$\tilde{\tilde{\boldsymbol{\beta}}}^T = \left[\tilde{\tilde{\beta}}(1),\ldots,\tilde{\tilde{\beta}}(m),..,\tilde{\tilde{\beta}}(N_b)\right] \tag{2.23a}$$

$$\tilde{\tilde{\boldsymbol{\theta}}}^T = \left[\tilde{\tilde{\theta}}(1),\ldots,\tilde{\tilde{\theta}}(m),..,\tilde{\tilde{\theta}}(N_b)\right] \tag{2.23b}$$

$\mathbf{\delta f^{\beta}_{F0}}, \mathbf{\delta f^{\theta}_{F0}}, \mathbf{\delta f^{\beta}_{F1}}$ and $\mathbf{\delta f^{\theta}_{F1}}$ are all row vectors of order N_b. In these vectors only the mth and nth terms are usually non-zero terms (in $\mathbf{\delta f^{\beta}_{F1}}$ the mth term is zero too). These line vectors are defined below:

$$\mathbf{\delta f^{\beta}_{F0}}(m,r,n,\rho,\nu)=\left[0,..,0,(r-e),0,..,0,-(\rho-e)\cdot e^{-i\cdot k\cdot\nu}\cdot e^{i\cdot k\cdot\psi(m,n)}\cdot[1-i\cdot k\cdot\xi_T(\rho)],0,..,0\right] \quad (2.24a)$$

(The term m ↓, The term n ↓)

$$\mathbf{\delta f^{\theta}_{F0}}(m,r,n,\rho,\nu)=\left[0,..,0,\ -s(r),0,..,0,-[\rho\cdot\xi_T(\rho)-s(\rho)]\cdot e^{-i\cdot k\cdot\nu}\cdot e^{i\cdot k\cdot\psi(m,n)}\cdot[1-i\cdot k\cdot\xi_T(\rho)],0,..,0\right] \quad (2.24b)$$

$$\mathbf{\delta f^{\beta}_{F1}}(m,r,n,\rho,\nu)=\left[0,..,0,\ 0\ \ -i\cdot k\cdot(\rho-e)\cdot e^{-i\cdot k\cdot\nu}\cdot e^{i\cdot k\cdot\psi(m,n)},0,..,0\right] \quad (2.24c)$$

$$\mathbf{\delta f^{\theta}_{F1}}(m,r,n,\rho,\nu)=\left[0,..,0,\ r,0,..,0,-i\cdot k[\rho\cdot\xi_T(\rho)-s(\rho)]\cdot e^{-i\cdot k\cdot\nu}\cdot e^{i\cdot k\cdot\psi(m,n)},0,..,0\right] \quad (2.24d)$$

As indicated by the underlined terms in Eq. (2.9c) $\mathbf{\delta f^{\theta}_{F0}}$ and $\mathbf{\delta f^{\theta}_{F1}}$ are small and thus can usually be neglected.

In order to calculate the aerodynamic loads it is necessary to calculate the function F(n,r,ξ,t) that represents the relative normal velocity, due to the blade motion, at the point (r,ξ) of the nth blade, at time t [12-14]. This function is defined as follows:

$$F(n,r,\xi,t)=\left.\frac{\partial f(n,r,\xi,\tau)}{\partial\tau}\right|_{\tau=t}-\Omega\frac{\partial f(n,r,\xi,t)}{\partial\xi} \quad (2.25)$$

Similar to the above derivations, the following expressions are used:

$$F(n,r,\xi,t)=\overset{\circ}{F}(r,\xi)+\tilde{F}(n,r,\xi,t) \quad (2.26a)$$

$$\tilde{F}(n,r,\xi,t)=\mathrm{Re}\left[\tilde{\tilde{F}}(n,r,\xi)\cdot e^{i\cdot\omega\cdot t}\right] \quad (2.26b)$$

If Eq. (2.6b) is substituted into Eq. (2.25) and Eqs. (2.11), (2.12) are also used, then the following expression for $\tilde{\tilde{F}}(n,r,\xi)$ is obtained:

$$\tilde{\tilde{F}}(n,r,\xi)=\tilde{\tilde{F}}_0(n,r)+\xi\cdot\tilde{\tilde{F}}_1(n,r) \quad (2.27a)$$

$$\tilde{\tilde{F}}_0(n,r)=\mathbf{F^{\beta}_0}(n,r)\cdot\tilde{\tilde{\boldsymbol\beta}}+\mathbf{F^{\theta}_0}(n,r)\cdot\tilde{\tilde{\boldsymbol\theta}} \quad (2.27b)$$

$$\tilde{\tilde{F}}_1(n,r)=\mathbf{F^{\beta}_1}(n,r)\cdot\tilde{\tilde{\boldsymbol\beta}}+\mathbf{F^{\theta}_1}(n,r)\cdot\tilde{\tilde{\boldsymbol\theta}} \quad (2.27c)$$

The vectors $\tilde{\tilde{\boldsymbol\beta}}$ and $\tilde{\tilde{\boldsymbol\theta}}$ were defined by Eqs. (2.23 a,b). $\mathbf{F^{\beta}_0}(n,r),\mathbf{F^{\theta}_0}(n,r),\mathbf{F^{\beta}_1}(n,r)$ and $\mathbf{F^{\theta}_1}(n,r)$ are row vectors of order N_b. All the terms of the vectors, $\mathbf{F^{\beta}_0}(n,r),\mathbf{F^{\theta}_0}(n,r)$, and $\mathbf{F^{\theta}_1}(n,r)$, except for the nth term, are equal to zero:

The term n
↓

$$\mathbf{F}_0^{\beta}(n,r) = [0,0,\ldots,0,i\cdot\omega\cdot(r-e),0,\ldots,0] \tag{2.28a}$$

⋮

$$\mathbf{F}_0^{\theta}(n,r) = [0,0,\ldots,0,-[\Omega\cdot r + i\cdot\omega\cdot s(r)],0,\ldots,0] \tag{2.28b}$$

⋮

$$\mathbf{F}_1^{\theta}(n,r) = [0,0,\ldots,\quad 0,\quad i\cdot\omega\cdot r,\quad 0,\ldots,0] \tag{2.28c}$$

$$\mathbf{F}_1^{\beta}(n,r) = [0] \tag{2.28d}$$

$\mathbf{F}_1^{\beta}(n,r)$ is included (although it is zero) for the ease of presenting the equations in the following derivations.

3. The Aerodynamic Loads

The lift force per unit length, at the cross-section r of blade m, at time τ, is denoted $L(m,r,\tau)$. Similar to the other variables, the lift force is described as follows:

$$L(m,r,\tau) = \overset{o}{L}(r) + \tilde{L}(m,r,\tau) \tag{3.1}$$

$$\tilde{L}(m,r,\tau) = \mathrm{Re}\left[\tilde{\tilde{L}}(m,r)\cdot e^{i\cdot\omega\cdot\tau}\right] \tag{3.2}$$

$\tilde{\tilde{L}}(m,r)$ is a complex amplitude that describes magnitude and phase shift.

As indicated above, the present aerodynamic calculations are based on the TEMURA model that is described in [12-14]. In this version of the model a constant circulation along the blade is assumed (that varies with time). The calculations are based on a representative cross-section of the blade, having a radial coordinate r_c. The lift forces (per unit length) at the representative cross-sections of all the blades are described by the following vector equation:

$$\tilde{\tilde{\mathbf{L}}}(r_c) = -2\cdot\pi\cdot\overset{*}{\rho}\cdot\Omega\cdot r_c^2\cdot\chi(r_c)\cdot\left(\mathbf{I}_{N_b}\cdot\mathbf{D_a}(r_c) + \mathbf{L_D}(r_c,k)\cdot\mathbf{D_e}(r_c)\right) \tag{3.3}$$

$\overset{*}{\rho}$ is the air mass density.

$$\chi(r_c) = c(r_c)/(2\cdot r_c) \tag{3.4}$$

where c(r) is the chord at cross-section r_c.

$\tilde{\tilde{\mathbf{L}}}(r_c)$ is a column vector of the order N_b that describes the complex amplitudes of the lift forces per unit length, at the cross-sections r_c of all the blades:

$$\tilde{\tilde{\mathbf{L}}}(r_c) = \left[\tilde{\tilde{L}}(1,r_c),\ldots,\tilde{\tilde{L}}(m,r_c),\ldots,\tilde{\tilde{L}}(N_b,r_c)\right]^T \tag{3.5}$$

$\mathbf{D_a}(r_c)$ and $\mathbf{D_e}(r_c)$ are column vectors of order N_b, that are the vectors of "equivalent" accelerations and "equivalent" velocities, respectively, at the cross-sections r_c of all the blades:

$$\mathbf{D_a}(r_c) = (i \cdot k'(r_c)/2) \cdot [D_0(1,r_c),\ldots,D_0(m,r_c),\ldots,D_0(N_b,r_c)]^T \tag{3.6}$$

$$\mathbf{D_e}(r_c) = [D_e(1,r_c),\ldots,D_e(m,r_c),\ldots,D_e(N_b,r_c)]^T \tag{3.7}$$

where:

$$k'(r_c) = k \cdot \chi(r_c) \tag{3.8}$$

$$D_e(n,r_c) = D_0(n,r_c) - \frac{1}{2} \cdot \chi(r_c) \cdot D_1(n,r_c) \tag{3.9}$$

$D_0(n,r_c)$ and $D_1(n,r_c)$ are defined below. $\mathbf{I_{N_b}}$ is a unit matrix of order N_b.

$\mathbf{L_D}(r_c,k)$ is the lift deficiency matrix. It is a circulant order of N_b [15], namely a square matrix that has a special circular form where all the elements on the diagonal are identical and the other elements of each row are shifted accordingly. The details of this matrix are given in [12,14].

The terms $D_0(n,r_c)$ and $D_1(n,r_c)$ represent "velocity" effects, and are defined by the following equation:

$$D_j(m,r) = \tilde{\tilde{F}}_j(m,r) - \frac{\mathring{\Gamma}_C}{4\pi} \sum_{n=1}^{n=N_b} [P_{GCj}(m,r,n,R_b) - P_{GCj}(m,r,n,R_a)] \qquad j=0,1 \tag{3.10}$$

$\mathring{\Gamma}_C$ is the cross-sectional circulation in the basic axisymmetric state (identical for all the blades).

The functions $P_{GCj}(m,r,n,\rho)$, for j = 0 or j = 1, are defined by the following equation (for more details see [12,13]):

$$P_{GCj}(m,r,n,\rho) = \int_{\nu=\psi(m,n)}^{\nu=\infty} V_{GC}(m,r,n,\rho,\nu) \cdot \delta\tilde{\tilde{f}}_{Fj}(m,r,n,\rho,\nu) \cdot d\nu \qquad j=0,1 \tag{3.11}$$

The function $V_{GC}(m,r,n,\rho,\nu)$ depends on the geometry of the wake in the basic state, and on the function $\delta \mathring{f}(r,\xi,\rho)$ as defined by Eq. (2.9b).

Substitution of Eqs. (2.22a,b) into Eq. (2.21), and then into Eq. (3.11), result in:

$$P_{GCj}(m,r,n,\rho) = \mathbf{P^{\beta}_{GCj}}(m,r,n,\rho) \cdot \tilde{\tilde{\boldsymbol{\beta}}} + \mathbf{P^{\theta}_{GCj}}(m,r,n,\rho) \cdot \tilde{\tilde{\boldsymbol{\theta}}} \qquad j=0,1 \tag{3.12}$$

$\mathbf{P^{\beta}_{GCj}}(m,r,n,\rho)$ and $\mathbf{P^{\theta}_{GCj}}(m,r,n,\rho)$, for j = 0 or j = 1, are row vectors of order N_b:

$$\mathbf{P}_{\mathbf{GCj}}^{\ell}(m,r,n,\rho)=\int_{\nu=\psi(m,n)}^{\nu=\infty}V_{GC}(m,r,n,\rho,\nu)\cdot\delta\mathbf{f}_{\mathbf{Fj}}^{\ell}(m,r,n,\rho,\nu)\cdot d\nu \qquad \mathbf{j}=0,1\ ;\ \ell=\beta,\theta \tag{3.13}$$

It should be noted that the last equations define four variables $\mathbf{P}_{\mathbf{GCj}}^{\ell}$ that represent all the possible combinations between $\mathbf{j}$ = 0,1 and ℓ = β,θ. Substitution of Eqs. (2.27b,c) and (3.12) into Eq. (3.10) results in the following expression for $D_j(m,r)$:

$$D_j(m,r)=\mathbf{D}_{\mathbf{j}}^{\beta}(m,r)\cdot\tilde{\tilde{\boldsymbol{\beta}}}+\mathbf{D}_{\mathbf{j}}^{\theta}(m,r)\cdot\tilde{\tilde{\boldsymbol{\theta}}} \qquad j=0,1 \tag{3.14}$$

$\mathbf{D}_{\mathbf{j}}^{\beta}(m,r)$ and $\mathbf{D}_{\mathbf{j}}^{\theta}(m,r)$ are row vectors of order N_b that are defined as:

$$\mathbf{D}_{\mathbf{j}}^{\ell}(m,r)=\mathbf{F}_{\mathbf{j}}^{\ell}(m,r)-\frac{\overset{\circ}{\Gamma}_c}{4\pi}\sum_{n=1}^{n=N_b}\left[\mathbf{P}_{\mathbf{GCj}}^{\ell}(m,r,n,R_b)-\mathbf{P}_{\mathbf{GCj}}^{\ell}(m,r,n,R_a)\right] \qquad \mathbf{j}=0,1\ ;\ \ell=\beta,\theta \tag{3.15}$$

It is convenient at this stage to define two new column vectors of order N_b:

$$\mathbf{D}_{\mathbf{j}}(r)=\left[D_j(1,r),..,D_j(m,r),..,D_j(N_b,r)\right]^T \qquad j=0,1 \tag{3.16}$$

Based on Eq. (3.14):

$$\mathbf{D}_{\mathbf{j}}(r)=\mathbf{D}_{\mathbf{j}}^{\beta}(r)\cdot\tilde{\tilde{\boldsymbol{\beta}}}+\mathbf{D}_{\mathbf{j}}^{\theta}(r)\cdot\tilde{\tilde{\boldsymbol{\theta}}} \qquad j=0,1 \tag{3.17}$$

where $\mathbf{D}_{\mathbf{j}}^{\beta}(r)$ and $\mathbf{D}_{\mathbf{j}}^{\theta}(r)$ are square matrices of order N_b, defined as:

$$\mathbf{D}_{\mathbf{j}}^{\ell}(r)=\begin{bmatrix}\mathbf{D}_{\mathbf{j}}^{\ell}(1,r)\\ \vdots\\ \mathbf{D}_{\mathbf{j}}^{\ell}(m,r)\\ \vdots\\ \mathbf{D}_{\mathbf{j}}^{\ell}(N_b,r)\end{bmatrix} \qquad \mathbf{j}=0,1\ ;\ \ell=\beta,\theta \tag{3.18}$$

It can be shown mathematically, and it is also supported by simple physical reasoning, that matrices $\mathbf{D}_{\mathbf{j}}^{\beta}(r)$ and $\mathbf{D}_{\mathbf{j}}^{\theta}(r)$ are circulants.

If Eq. (3.17) is used, then according to Eqs. (3.6)-(3.9):

$$\mathbf{D}_{\mathbf{a}}(r_c)=\left(i\cdot k'(r_c)/2\right)\left[\mathbf{D}_0^{\beta}(r_c)\cdot\tilde{\tilde{\boldsymbol{\beta}}}+\mathbf{D}_0^{\theta}(r_c)\cdot\tilde{\tilde{\boldsymbol{\theta}}}\right] \tag{3.19}$$

$$\mathbf{D}_{\mathbf{e}}(r_c)=\mathbf{D}_{\mathbf{0}}^{\beta}(r_c)\cdot\tilde{\tilde{\boldsymbol{\beta}}}+\mathbf{D}_{\mathbf{0}}^{\theta}(r_c)\cdot\tilde{\tilde{\boldsymbol{\theta}}}-\frac{1}{2}\cdot\chi(r_c)\cdot\left[\mathbf{D}_{\mathbf{1}}^{\beta}(r_c)\cdot\tilde{\tilde{\boldsymbol{\beta}}}+\mathbf{D}_{\mathbf{1}}^{\theta}(r_c)\cdot\tilde{\tilde{\boldsymbol{\theta}}}\right] \tag{3.20}$$

Substitution of Eq. (3.20) into Eq. (3.3) results in the following equation for the vector of cross-sectional lifts.

$$\tilde{\tilde{L}}(r_c) = -2\pi \cdot \overset{*}{\rho} \cdot \Omega \cdot r_c^2 \cdot \chi(r_c) \cdot \left[\mathbf{L}_\beta(r_c, k) \cdot \tilde{\tilde{\beta}} + \mathbf{L}_\theta(r_c, k) \cdot \tilde{\tilde{\theta}} \right] \tag{3.21}$$

$\mathbf{L}_\beta(r_c, k)$ and $\mathbf{L}_\theta(r_c, k)$ are square matrices of order N_b:

$$\mathbf{L}_\ell(r_c, k) = \left(i \cdot k'(r_c)/2\right) \cdot \mathbf{D}_0^\ell(r_c)$$

$$+\mathbf{L}_\mathbf{D}(r_c, k) \cdot \left[\mathbf{D}_0^\ell(r_c) - \frac{1}{2} \cdot \chi(r_c) \cdot \mathbf{D}_1^\ell(r_c) \right] \qquad \ell = \beta, \theta \tag{3.22}$$

Since addition, subtraction and multiplication of circulants result in circulants [15], it is clear that $\mathbf{L}_\beta(r_c, k)$ and $\mathbf{L}_\theta(r_c, k)$ are also circulants. This circulatory nature is supported again by simple physical reasoning.

The flapping moment of the aerodynamic forces acting on blade m, about the flapping hinge, at time τ, $M_{A\beta}(m,\tau)$, is defined as:

$$M_{A\beta}(m, \tau) = \int_{\rho=e}^{\rho=R} (\rho - e) \cdot L(m, \rho, \tau) \cdot d\rho \tag{3.23}$$

R is the radius of the rotor ($R \equiv R_b$).

Similar to the above derivations, $M_{A\beta}(n,\tau)$ can be described as follows:

$$M_{A\beta}(n, \tau) = \overset{\circ}{M}_{A\beta} + \tilde{M}_{A\beta}(n, \tau) \tag{3.24}$$

$$\tilde{M}_{A\beta}(n, \tau) = \mathrm{Re}\left[\tilde{\tilde{M}}_{A\beta}(n) \cdot e^{i \cdot \omega \cdot \tau} \right] \tag{3.25}$$

Substitution of Eqs. (3.1) and (3.2) into Eqs. (3.23), and using for the integration the approximation of [12,14], lead to the following expression for $\tilde{\tilde{M}}_{A\beta}(n)$:

$$\overset{\circ}{M}_{A\beta} \cong R^2 \cdot k_{m\beta}(e/R) \cdot \overset{\circ}{L}(0.75R) \tag{3.26a}$$

$$\tilde{\tilde{M}}_{A\beta}(m) \cong R^2 \cdot k_{m\beta}(e/R) \cdot \tilde{\tilde{L}}(m, 0.75R) \tag{3.26b}$$

$$k_{m\beta}(e/R) = 0.46 - 0.63 \cdot (e/R) \tag{3.26c}$$

It is convenient to define the vector of perturbations in the aerodynamic flapping moments as follows:

$$\tilde{\tilde{\mathbf{M}}}_{\mathbf{A\beta}} = \left[\tilde{\tilde{M}}_{A\beta}(1), .., \tilde{\tilde{M}}_{A\beta}(m), .., \tilde{\tilde{M}}_{A\beta}(N_b) \right]^T \tag{3.27}$$

According to Eqs. (3.21), (3.26b) and (3.27), and after substituting 0.75R for r_c, one obtains:

$$\tilde{\tilde{\mathbf{M}}}_{A\beta} = -\left[9\pi \cdot \overset{*}{\rho} \cdot \Omega \cdot R^4 \cdot \chi(0.75R) \cdot k_{m\beta}(e/R)/8\right]\left[\mathbf{L}_\beta(0.75R,k) \cdot \tilde{\tilde{\beta}} + \mathbf{L}_\theta(0.75R,k) \cdot \tilde{\tilde{\theta}}\right] \tag{3.28}$$

The rotor thrust at any moment, $T(\tau)$, is defined as:

$$T(\tau) = \sum_{n=1}^{n=N_b} \int_{\rho=e}^{\rho=R} L(n,\rho,\tau) \cdot d\rho \tag{3.29}$$

Similar to the other variables, $T(\tau)$ can be described as follows:

$$T(\tau) = \overset{o}{T} + \tilde{T}(\tau) \tag{3.30}$$

$$\tilde{T}(\tau) = Re\left[\tilde{\tilde{T}} \cdot e^{i \cdot \omega \cdot \tau}\right] \tag{3.31}$$

Following a procedure similar to the one that led to Eq. (3.28), the following expression is obtained (for details see [12]):

$$\overset{o}{T} = 0.63 \cdot N_b \cdot R \cdot \overset{o}{L}(0.75R) \tag{3.32a}$$

$$\tilde{\tilde{T}} = -\left[9\pi \cdot \overset{*}{\rho} \cdot \Omega \cdot R^3 \cdot \chi(0.75R) \cdot 0.63/8\right] \left[\overbrace{1,1,\ldots,1}^{N_b \text{ terms}}\right]$$

$$\cdot\left[\mathbf{L}_\beta(0.75R,k) \cdot \tilde{\tilde{\beta}} + \mathbf{L}_\theta(0.75R,k) \cdot \tilde{\tilde{\theta}}\right] \tag{3.32b}$$

4. The Flapping Equation

4.1 General derivation

The flapping equation of blade m is:

$$I \cdot \ddot{\beta}(m,t) + 2 \cdot \zeta \cdot \omega_f \cdot I \cdot \dot{\beta}(m,t) + \omega_f^2 \cdot I \cdot \beta(m,t) = M_{A\beta}(m,t) \tag{4.1a}$$

$$\omega_f^2 = (1 + e \cdot K/I) \cdot \Omega^2 + k_f/I \tag{4.1b}$$

I is the blade mass moment of inertia about the flapping hinge. K is the first mass moment of inertia about the same hinge. k_f is a torsional flapping spring about the flapping hinge. ω_f is the natural frequency of flapping of the rotating blade. ζ is the mechanical viscous damping ratio of the blade flapping.

Substitution of the expressions for $\beta(m,t)$ and $M_{A\beta}(m,t)$ into Eq. (4.1), results in two flapping equations: one for the basic state and one for the perturbation (for more details see [14]).

Solution of the flapping equation for the basic state results in the following expression for $\overset{o}{\beta}$:

$$\overset{o}{\beta} = R \cdot k_{m\beta}(e/R) \cdot \overset{o}{T} \Big/ \left(0.63 \cdot N_b \cdot I \cdot \omega_f^2\right) \tag{4.2}$$

The perturbation equation, after division by $\left(I \cdot \Omega^2\right)$, becomes:

$$\left(\omega_f^2/\Omega^2 - k^2 + 2 \cdot i \cdot \zeta \cdot k \cdot \omega_f/\Omega\right) \cdot \tilde{\tilde{\beta}}(m) = \tilde{\tilde{M}}_{A\beta}(m) \Big/ \left(I \cdot \Omega^2\right) \tag{4.3}$$

If Eq. (3.28) is used, then Eq. (4.3) becomes:

$$\mathbf{E}_\beta(0.75R, k) \cdot \tilde{\tilde{\boldsymbol{\beta}}} = \mathbf{E}_\theta(0.75R. k) \cdot \tilde{\tilde{\theta}} \tag{4.4}$$

$\mathbf{E}_\beta(0.75R, k)$ and $\mathbf{E}_\theta(0.75R, k)$ are circulants of order N_b, defined as:

$$\mathbf{E}_\beta(0.75R, k) = \left(\omega_f^2/\Omega^2 - k^2 + 2 \cdot i \cdot \zeta \cdot k \cdot \omega_f/\Omega\right) \cdot \mathbf{I}_{N_b}$$

$$+\left[3 \cdot \gamma \cdot k_{m\beta}(e/R)/(8 \cdot \Omega \cdot R)\right] \cdot \mathbf{L}_\beta(0.75R, k) \tag{4.5}$$

$$\mathbf{E}_\theta(0.75R, k) = -\left[3 \cdot \gamma \cdot k_{m\beta}(e/R)/(8 \cdot \Omega \cdot R)\right] \cdot \mathbf{L}_\theta(0.75R, k) \tag{4.5b}$$

γ is the Lock number, based on the the chord at 0.75R cross-section, defined as:

$$\gamma = 3 \cdot \overset{*}{\rho} \cdot \pi \cdot R^5 \cdot \chi(0.75R)/I \tag{4.6}$$

$\tilde{\tilde{\theta}}$ is the forcing function that is considered as an input to the problem. In what follows two cases will be considered: collective pitch variations and differential pitch variations.

4.2 Collective pitch variations

In this case the pitch variations of all the blades are identical without any phase shift. It is clear that the flapping response of all the blades will be identical. Thus, it can be written:

$$\tilde{\tilde{\theta}} = \mathbf{U}\, \theta_{col} \tag{4.7a}$$

$$\tilde{\tilde{\boldsymbol{\beta}}} = \mathbf{U}\, \beta_{col} \tag{4.7b}$$

U is a column vector of order N_b where all the elements are unity.

All the N_b Eqs. (4.4) are identical in this case and therefore it is possible to use only one equation. Thus Eq. (4.4) becomes:

$$[1,0,\ldots,0] \cdot \mathbf{E}_\beta(0.75R, k) \cdot \mathbf{U} \cdot \beta_{col} = [1,0,\ldots,0] \cdot \mathbf{E}_\theta(0.75, k) \cdot \mathbf{U} \cdot \theta_{col} \tag{4.8}$$

4.3 Differential pitch variations

In this case all the blades execute harmonic pitch variations with the same amplitude and a phase shift angle, between consequent blades, of $(2\pi/N_b)$. Thus:

$$\tilde{\tilde{\theta}} = \mathbf{S}\,\theta_d \qquad (4.4)$$

S is a vector of order N_b, defined as:

$$\mathbf{S} = \begin{bmatrix} 1 \\ \vdots \\ e^{i\cdot 2\cdot\pi/N_b} \\ \vdots \\ e^{i\cdot 2\cdot\pi\cdot(N_b-1)/N_b} \end{bmatrix} \qquad (4.10)$$

Because of physical reasoning, it is clear that the flapping response will also be:

$$\tilde{\tilde{\beta}} = \mathbf{S}\cdot\beta_d \qquad (4.11)$$

Substitution of Eqs. (4.10) and (4.11) into Eq. (4.4), and taking only the first equation, results in:

$$[1,0,\ldots,0]\cdot\mathbf{E}_\beta(0.75R,k)\cdot\mathbf{S}\cdot\beta_d = [1,0,\ldots,0]\cdot\mathbf{E}_\theta(0.75,k)\cdot\mathbf{S}\cdot\theta_d \qquad (4.12)$$

5. Results

In order to validate the new model it is applied to analyse two cases that were reported in the literature [1,2 and 9] and where experimental results also exist.

5.1 Single-bladed rotor (Ref. 9)

The blade in this case was a hingeless blade that was rotated at a constant speed of Ω=360 r.p.m.

The blade pitch was varied (harmonic variations) about a certain basic pitch angle, $\overset{o}{\theta}$. The frequency of these variations ranged between very small values and five times the frequency of the rotor rotation. The vertical hub force was measured by strain-gages.

Because a single blade is considered, the cases of collective pitch variations (Subsecton 4.2) and differential pitch variations (Subsection 4.3) coincide. Since the next example includes differential pitch variations, this case will be dealt with as collective pitch variations.

Based on the properties of the hingeless blade, as presented in [9], an approximate equivalent "rigid-model" was constructed by choosing appropriate values of: I, K, e and k_f.

In [9] experimental results of the amplitude ratio and phase shift between the harmonic variations in the rotor thrust coefficient and the variations of the blade pitch angle were presented, for two values of the pitch angles of the blades basic state ($\overset{\circ}{\theta} = 0°, 6°$). In Figs. 1 and 2 these experimental results are compared with theoretical results of the present model. Because of certain numerical problems in running the case of $\overset{\circ}{\theta} = 0°$, the numerical results are for $\overset{\circ}{\theta} = 1°$. It should be noted that in the experiment the strain gages measure the resultant force that include aerodynamic and dynamic contributions. Thus inertia contributions should be added to the aerodynamic contributions that are given by Eq. (3.32b). These inertial contributions to the thrust force, for the present theoretical model, are $-K\ddot{\tilde{\beta}}$.

The experimental results for $\overset{\circ}{\theta} = 0°$ (Fig. 1) show very clearly the influence of the returning wake behind the blade. In the neighborhood of integer multiples of the rotor angular speed (k=1,2,3) there are relatively sharp variations in the amplitude ratio and phase shift. These sharp variations are also clearly shown in the theoretical results (Loewy's model presents similar trends in [9]). In addition there is a very good agreement in the resonance behavior, at k=2.48, between the experimental results and the results of the new theoretical model. While there is in general a good agreement between the experimental and theoretical results, certain deviations exist. At low frequencies, in addition to certain shifts between the theoretical and experimental results, it is evident that the phase variations near integer values of k are sharper in the experiment than in the theoretical results. Numerical investigation has shown that the theoretical results become sharper as $\overset{\circ}{\theta}$ is decreased towards zero. Since (as indicated above) decreasing $\overset{\circ}{\theta}$ towards zero causes numerical problems, it was decided to present results for $\overset{\circ}{\theta} = 1°$ (further discussion will appear in [16]). There are also deviations between the experimental and theoretical results at high frequencies (k>3). It seems that at these frequencies the approximation of the hingeless elastic blade, by an offset flapping hinge and a flapping spring, is problematic.

In Fig. 2 results for $\overset{\circ}{\theta} = 6°$ are presented. The general trend is similar to that of Fig. 1. Because of the fact that the wake departs from the rotor faster than in the case of Fig. 1, wake influences are less pronounced. Thus the sharp variations in the case of integer values of k, almost disappear in the experimental results. While these shape variations are also reduced in the case of the theoretical results, they are still larger compared to the experimental results.

5.2 Two-bladed rotor (Refs. 1,2)

A two-bladed hingeless rotor is considered. The details of the experimental model are presented in [1,2]. Again, these hingeless elastic blades are approximated by equivalent rigid blades having appropriate values of: e, K, I and k_f. Since this experiment is confined to low frequencies (relative to the experiment of [9]), this approximation gives very good results. In this experiment differential pitch variations are considered (see Subsection 4.3). Two cases of basic pitch angles are investigated: $\overset{\circ}{\theta} = 2°$ and 8°. Results for the case of $\overset{\circ}{\theta} = 2°$ are presented in Fig. 3. In the figure the amplitude ratio and phase shift between the flapping angle response and the differential pitch variation are presented. In addition to the experimental results and numerical results of the present new model, results of a quasi-steady aerodynamic blade-element model are presented. A very good agreement between the results of the present new model and the experimental results is shown. It is also shown that large deviations exist, in large regions of frequency ratio k, between the results of the blade-element model and the other results.

The results for $\mathring{\theta} = 8°$ are presented in Fig. 4. While the results are similar to those of Fig. 3, the unsteady aerodynamic influences are somewhat reduced and therefore the differences between the new unsteady model and the blade-element model are slightly reduced. Again the agreement between the results of the new model and the experimental results is very good, although somewhat worse than in the case of $\mathring{\theta} = 2°$.

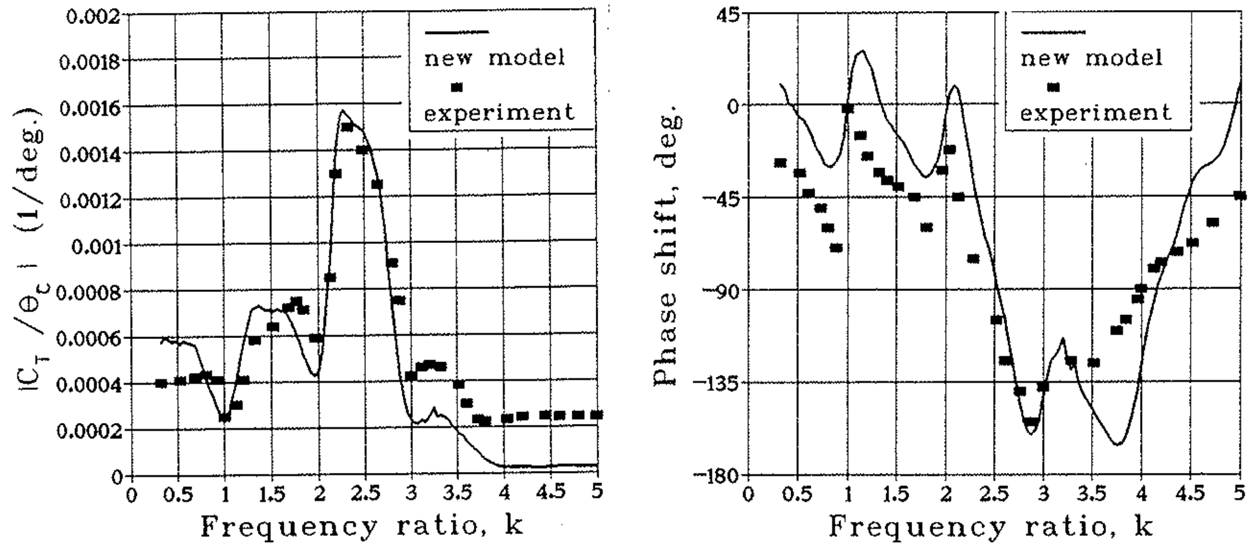

Fig. 1: Single-bladed rotor: Amplitude ratio and phase shift between the thrust coefficient variations and pitch angle variations. $\mathring{\theta} = 0°$ in the experiment and $\mathring{\theta} = 1°$ in the numerical results.

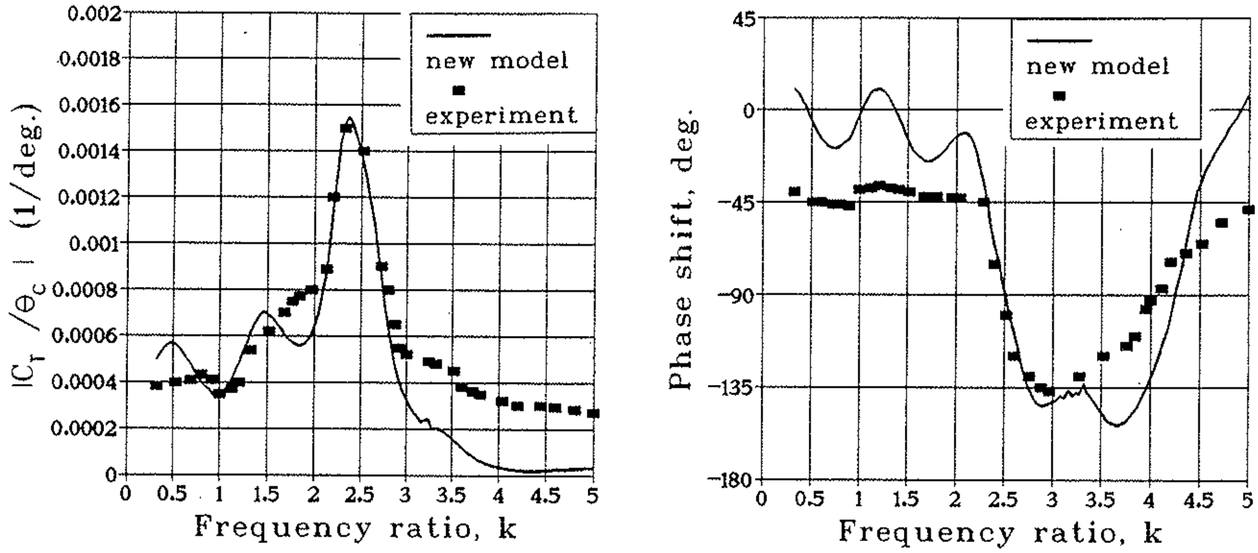

Fig. 2: Single-bladed rotor: Amplitude ratio and phase shift between the thrust coefficient variations and pitch angle variations. $\mathring{\theta} = 6°$.

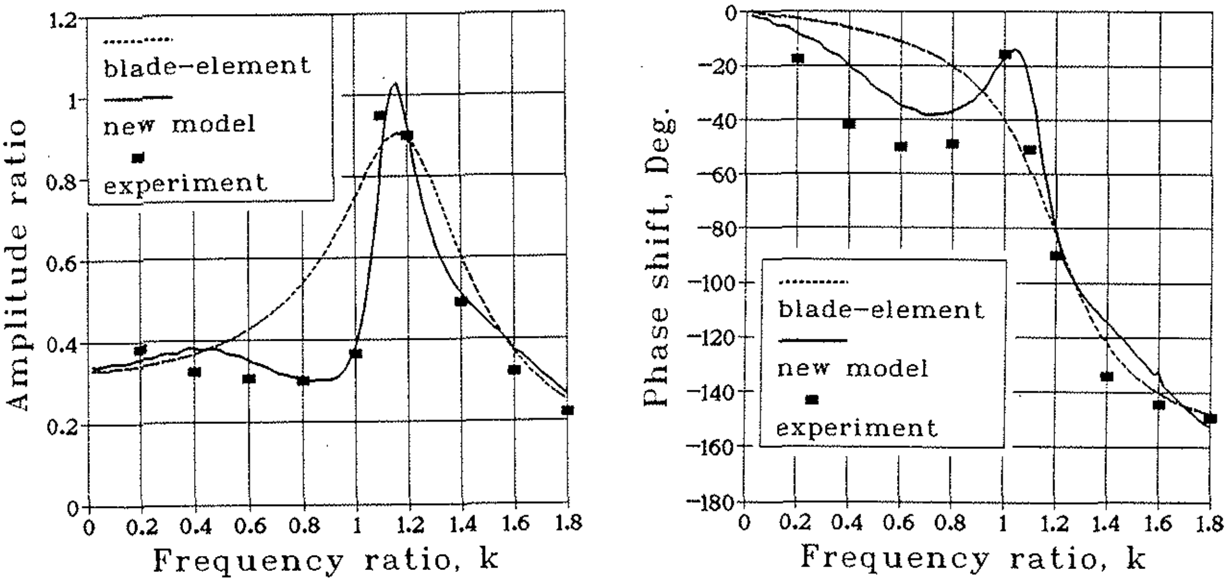

Fig. 3: Two-bladed rotor: Amplitude ratio and phase shift between the flapping angle response and pitch angle variations, $\mathring{\theta} = 2°$.

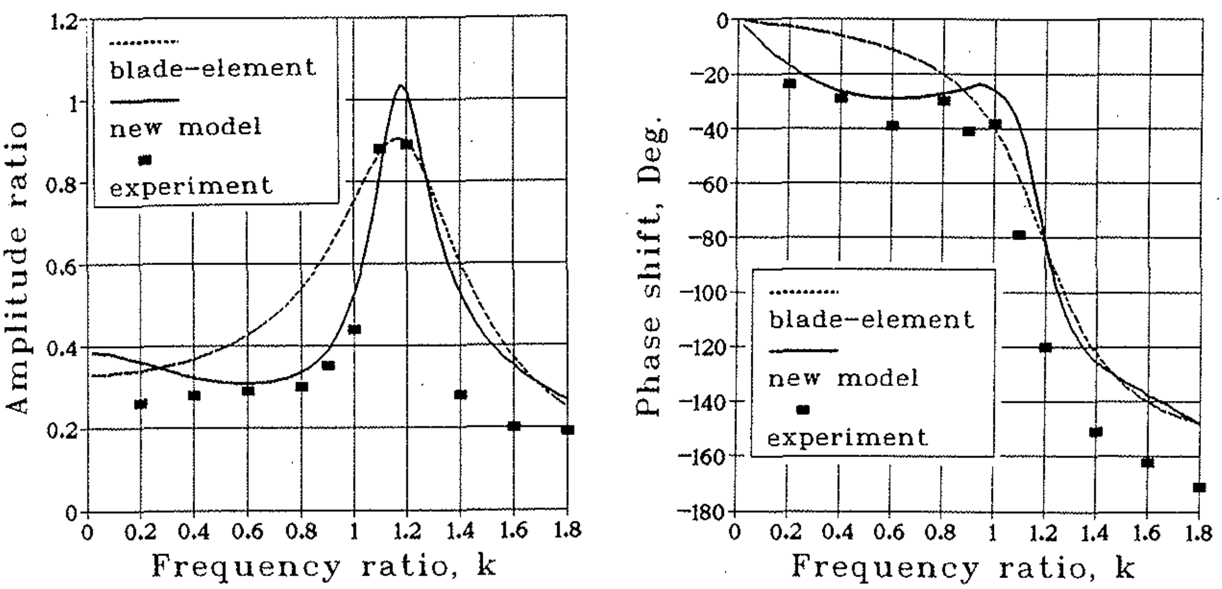

Fig. 4: Two-bladed rotor: Amplitude ratio and phase shift between the flapping angle response and pitch angle variations, $\mathring{\theta} = 8°$.

6. Conclusions

A new model for calculating the flapping response of rotor blades to harmonic variations of their pitch angles, for a hovering rotor or a rotor in axial flight, has been presented. This model is based on an unsteady aerodynamic model, named TEMURA, that has been developed in the Technion during recent years. This model is a three-dimensional aerodynamic model that takes into account the influence of shed and trailing vortices, together with geometric effects due to the spatial motion of the blades, that influence the wake geometry. The model includes a detailed inter-blade aerodynamic coupling.

Comparison between the numerical results of the new model and experimental results from the literature shows that the agreement is significantly improved as a result of including the unsteady effects and inter-blade aerodynamic coupling. Because of the lack of space only limited results have been presented. A more detailed investigation will be presented in a future paper [16].

References

[1] K.H. Hohenemser and S.T. Crews, "Model Tests on Unsteady Rotor Wake Effects", *J. of Aircraft*, Vol. 10, No. 1, 1973, pp. 58-60.

[2] S.T. Crews and K.H. Hohenemser, "An Unsteady Wake Model for a Hingeless Rotor", *J. of Aircraft*, Vol. 10, No. 12, 1973, pp. 758-760.

[3] G.J. Sissingh, "The Effect of Induced Velocity Variation on Helicopter Rotor Damping in Pitch or Roll", *Aeronautical Research Council Paper* No. 101, Technical Note. No. Aero. 2132, November 1952.

[4] H.C., Curtiss, Jr. and N.K. Shupe, "A Stability and Control Theory for Hingeless Rotors", *Annual National Forum of the American Helicopter Society*, Washington, D.C., 1971.

[5] R.A. Ormiston, and D.A. Peters, "Hingless Helicopter Rotor Response with Non-Uniform Inflow and Elastic Blade Bending", *J. of Aircraft*, Vol. 9, No. 10, 1972, pp. 730-736.

[6] D.M. Pitt, D.M. and D.A. Peters, "Theoretical Prediction of Dynamic Inflow Derivatives", *Vertica*, Vol. 5, No. 1, 1981, pp. 21-34.

[7] G.H. Gaonkar, and D.A. Peters, D.A., "Review of Dynamic Inflow Modeling for Rotorcraft Flight Dynamics", *Vertica*, Vol. 12, No. 3, 1988, pp. 213-242.

[8] D.A. Peters, D.D. Boyd, and C.J. He, "Finite-State Induced-Flow Model for Rotors in Hover and Forward Flight", *J. of the Am. Helicopter Soc.*, Vol. 34, No. 4, 1989, pp. 5-17.

[9] T. Nagashima, G. Hasegawa, T. Nekohashi, and T. Hirose, "Aeroelastic Response Characteristics of a Rotor Executing Arbitrary Harmonic Blade Pitch Variations", *14th European Rotorcraft Forum*, Milano, Italy, 20-23 September, 1988, Paper no. 61.

[10] R.G. Loewy, "A Two-Dimensional Approximation to the Unsteady Aerodynamics of Rotary Wings", *J. of the Aeronautical Sciences*, Vol. 24, No. 2, 1957, pp. 81-92.

[11] R.H. Miller, "Rotor Blade Harmonic Air Loading", *AIAA J.*, Vol. 2, No. 7, 1964, pp. 1254-1269.

[12] A.Rosen, and A. Isser, "The Influence of Variations in the Blades' Locations on the Loads of a Helicopter Rotor During Perturbations About an Axial Flight", TAE Report, No. 721 *Faculty of Aerospace Engineering, Technion - Israel Institute of Technology*, Haifa, Israel, October 1994.

[13] A.Isser, and A. Rosen, "A Model of the Unsteady Aerodynamics of a Hovering Helicopter Rotor that Includes Variations in the Wake Geometry", *34th Israel Annual Conference on Aerospace Sciences*, February 16-17, 1994, pp. 90-105. Has also been submitted for publication.

[14] A. Rosen, and A. Isser, "A New Model of Rotor Dynamics During Pitch and Roll of a Hovering Helicopter", *Proceedings of the 50th Annual Forum of the American Helicopter Society*, Washington, DC, May 11-13, 1994. has also been submitted for publication.

[15] F.A. Graybill, *Matrices with Applications in Statistics*, Wadsworth Inc. 1983.

[16] A. Isser and A. Rosen, "A Study of the Flapping Response of Blades of a Hovering Helicopter to Harmonic Variatons of Their Pitch Angles", in preparation.